Proceedings of the 20th International Conference on Soil Mechanics and Geotechnical Engineering– Rahman and Jaksa (Eds)

Assessment of liquefaction triggering by seismic dilatometer tests: comparison between semi-empirical approaches and non-linear dynamic analyses

Évaluation du déclenchement de la liquéfaction par des essais au dilatomètre sismique: comparaison entre approches semi-empiriques et analyses dynamiques non-linéaire

Anna Chiaradonna & Paola Monaco

Department of Civil, Construction-Architectural and Environmental Engineering, University of L'Aquila, Italy, anna.chiaradonna1@univaq.it

ABSTRACT: The evaluation of soil liquefaction potential can be assessed using approaches with an increasing level of complexity. In engineering practice, the most common method is based on the use of empirical charts where the soil cyclic resistance is correlated to the soil resistance as measured in field tests, such as standard penetration test (SPT) and cone penetration test (CPT). Similarly, also seismic dilatometer tests (SDMT) can be used to assess the potential triggering of liquefaction in soil deposits as already shown in several case studies in Italy and around the world. In the present study, the results of seismic dilatometer tests carried out along a sketch of a river dyke highly damaged by the 2012 Emilia Earthquake have been used to assess the liquefaction potential of the embankment and the foundation deposits, using semi-empirical methods and dynamic analysis. Both methodologies highlighted high liquefaction risk for the investigated soils which is also compatible with the results obtained by more sophisticated non-linear dynamic analysis of the dyke carried out in effective stress condition. Finally, the advantages and limitations of the adopted approaches are discussed and practical guidelines are provided for SDMT-based methods.

RÉSUMÉ: Le potentiel de liquéfaction des sols peut être évalué à l'aide d'approches de complexité croissante. Dans la pratique de l'ingénierie, la méthode la plus courante est basée sur l'utilisation de chartes empiriques où la résistance cyclique du sol est corrélée à des paramètres mesurés lors d'essais au terrain, tels que l'essai de pénétration standard (SPT) ou le cône de pénétration standard (CPT). De la même manière, le dilatomètre sismique (SDMT) peut être utilisé pour évaluer le potentiel de liquéfaction dans les dépôts de sol, comme il a déjà été démontré montré dans plusieurs études de cas en Italie et dans le monde. Dans la présente étude, les résultats d'essais au dilatomètre sismique effectués le long d'une esquisse d'une digue fluviale fortement endommagée par le séisme d'Emilia en 2012 ont été utilisés pour évaluer le potentiel de liquéfaction du remblai et de la fondation, en utilisant des méthodes semi-empiriques et des analyses dynamiques. Les deux méthodologies ont mis en évidence un risque élevé de liquéfaction des sols à l'étude tout en démontant la compatible avec des résultats obtenus par une analyse dynamique non linéaire plus sophistiquée de la digue réalisée en contraintes effectives. Finalement, les avantages et les limites des approches adoptées sont discutés et des directives pratiques sont fournies pour les méthodes basées sur SDMT.

KEYWORDS: dilatometer test, cone penetration test, liquefaction, empirical chart, model calibration.

1 INTRODUCTION

Liquefaction caused significant damage to engineered structures and lifelines during recent earthquakes (2011 Christchurch, New Zealand earthquake; 2018 Palu, Indonesia earthquake; 2020 Petrinja, Croatia earthquake). This is the reason why an accurate prediction of the liquefaction potential is becoming a fundamental requirement for assessing the seismic safety and resilience of structures and infrastructures in saturated soils. The impossibility to retrieve undisturbed samples of liquefiable soils, at least with conventional equipment, makes the assessment of the liquefaction potential of soils largely based on field investigations, such as the Standard Penetration Test (SPT) and Cone Penetration Test (CPT). Similarly, also Dilatometer (DTM) or Seismic Dilatometer Tests (SDMT) can be used to assess the potential triggering of liquefaction in soil deposits as already shown in several case studies in Italy and around the world (Monaco et al. 2011, 2016; Amoroso et al. 2014, 2015, 2017, 2018, 2020; Boncio et al. 2018; Porcino et al. 2019; Monaco and Amoroso 2019). This latter case has the additional advantage to allow the evaluation of the soil liquefaction potential through the direct measurement of both the shear wave velocity, V_S, and the horizontal stress index K_D (often alternatively called stress history index). While the V_S-based estimation follows the general framework proposed by Andrus and Stokoe (2000), without specific concerns related to the specific test, the stress index approach required the development of an "*ad-hoc*" one-to-one empirical relationship between the Cyclic Resistance Ratio (CRR) and K_D (Monaco et al. 2005; Robertson 2012; Marchetti 2016).

This study proposes an updating empirical curve for DMT, following the framework providing by Boulanger and Idriss (2014), which includes data obtained from recent events where widespread liquefaction was observed (the 2010-2011 Canterbury earthquake sequence in New Zealand and the 2011 Tohoku earthquake in Japan).

The performance of the proposed curve is compared with that obtained by CPT results along with a sketch of a river dyke highly damaged by the 2012 Emilia Earthquake.

Moving to a more sophisticated approach, the proposed K_D-based empirical curve has been used to calibrate a simplified model for predicting the pore water pressure build-up induced by seismic loading, following a prompt calibration process for effective stress analysis already proposed by several researchers (Ntritos and Cubrinovski 2020; Chiaradonna et al. 2020).

Both methodologies highlighted high liquefaction risk for the investigated foundation soil deposits of the dyke which are also compatible with the observed damage pattern. Finally, the advantages and limitations of the adopted approaches are discussed and practical guidelines are provided for DMT or SDMT-based methods.

2 METHODOLOGY

According to Boulanger and Idriss (2014), CPT results are expressed in terms of corrected cone tip resistance, q_{c1Ncs}. The corrected cone tip resistance, q_{c1Ncs} is defined as:

$$q_{c1Ncs} = q_{c1N} + \Delta q_{c1N} \tag{1}$$

where:

$$q_{c1N} = C_N \cdot \frac{q_c}{P_a} \tag{2}$$

$$C_N = \left(\frac{P_a}{\sigma'_v}\right)^m \leq 1.7 \tag{3}$$

$$m = 1.338 - 0.249 \cdot q_{c1Ncs}^{0.264} \tag{4}$$

$$\Delta q_{c1N} = \left(11.9 + \frac{q_{c1N}}{14.6}\right) \exp\left(1.63 - \frac{9.7}{FC+2} - \left(\frac{15.7}{FC+2}\right)^2\right) \tag{5}$$

where q_c is the cone resistance measured during CPT, P_a is the atmospheric pressure and FC is the fines content, i.e., the percentage of soil having particles diameter smaller than 0.075 mm. The value of q_{c1Ncs} must be found by trial and error.

Differently from previous studies (e.g., Robertson 2012), the q_{c1Ncs} is the only variable that will be used in the following to correlate CPT to DMT or SDMT data.

Finally, the CPT-based empirical relationship proposed by Boulanger and Idriss (2014) is the following:

$$CRR_{M=7.5,\sigma'=1} = \exp\left(\frac{q_{c1Ncs}}{113} + \left(\frac{q_{c1Ncs}}{1000}\right)^2 - \left(\frac{q_{c1Ncs}}{140}\right)^3 + \left(\frac{q_{c1Ncs}}{137}\right)^4 - 2.8\right) \tag{6}$$

Eq. (6) provides the cyclic resistance ratio of the soil characterized by a given value of q_{c1Ncs} at a reference earthquake of 7.5 magnitude and effective overburden stress equal to unity. Further corrections to Eq. (6) are necessary to take into account: (i) the overburden stress, via the correction factor K_σ, and (ii) the actual magnitude and duration of the earthquake, via the Magnitude Scaling Factor, MSF. Additional details can be found in Boulanger and Idriss (2014).

2.1 *Updating the evaluation of the cyclic soil strength based on dilatometer test*

To update the cyclic strength estimation based on flat dilatometer to the most recent framework proposed by Boulanger and Idriss (2014), the horizontal stress index K_D has been correlated to q_{c1Ncs}. The field investigation data reported by Tsai et al. (2009) for 5 different sites in Taiwan have been digitalized and re-interpreted according to the following procedure. Cone tip resistance data related to a soil behaviour type (I_c) between 1.5 and 2.6 has been considered, while data outside this range has been neglected. An estimation of the fines content equal to 10% has been adopted for the calculation of Δq_{c1N}, and the final q_{c1Ncs} values have been obtained based on the water table depths and soil unit weights reported by Tsai et al. (2009) for each site. Due to the remarkable number of fines, site 3 has been excluded from the computations.

The calculated q_{c1Ncs} values are correlated to the measurements of K_D by Tsai et al. (2009) in Figure 1. Despite the dispersion, the dataset can be well described by a linear trend with a slope of 20, similarly to the approach proposed by Robertson (2012).

The same figure reports also another set of data related to the Scortichino site (Italy), where both CPT and SDMT were performed (Tonni et al. 2015). The second dataset has been processed according to the same protocol (only FC<10%), and it is better interpreted by a linear trend with a slope of about 30.

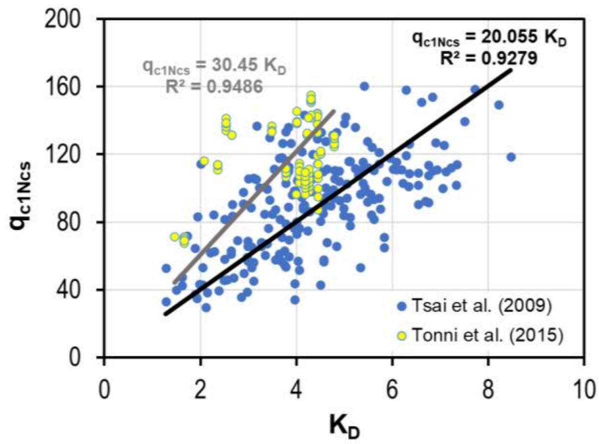

Figure 1. Relationship between q_{c1Ncs} and K_D.

Due to the discrepancy in the two considered datasets and considering also the limited amount of processed data, an average coefficient of 25 has been adopted, which is also compatible with the relationship reported by Marchetti (2016):

$$q_{c1Ncs} = 25K_D \tag{7}$$

By substituting the Eq. (7) into the Eq. (6) proposed by Boulanger and Idriss (2014), the final relationship is obtained:

$$CRR = \exp(0.001109K_D^4 - 0.00569K_D^3 + 0.000625K_D^2 + 0.221K_D - 2.8) \tag{8}$$

Differences between Eq. (8) and the most recent DMT-based curve proposed in the literature are observed for K_D lower than 3 and higher than 6 (Figure 2).

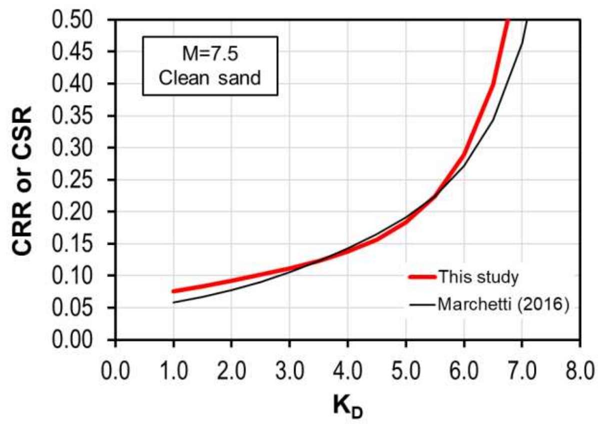

Figure 2. Relationship between CRR and K_D compared with the previous curve proposed by Marchetti (2016).

3 APPLICATION

The proposed DMT empirical relationship (Eq. 8) has been applied to an Italian case study located in Scortichino (Emilia, Italy), where significant evidence of soil deformation and building damages were observed after the Mw 6.1 earthquake of 20.V.2012 (Tonni et al. 2015).

Firstly, the liquefaction potential of soils has been evaluated through simplified procedures, based on the CPT and SDMT profiles.

Then, an effective stress dynamic analysis has been carried out by adopting the Eq. (8) for the calibration of the cyclic strength of the liquefiable deposit in the numerical model.

3.1 *Liquefaction assessment by using CPT*

The analyses have been executed using the simplified approach proposed by Boulanger and Idriss (2014), based on the comparison, at any depth, of the seismic demand on a soil layer generated by the earthquake (cyclic stress ratio CSR) and the capacity of the soil to resist liquefaction (cyclic resistance ratio CRR). When CSR is greater than CRR liquefaction may occur. CSR has been calculated with the usual expression:

$$CSR = 0.65\frac{\tau_{max}}{\sigma'_v} = 0.65\frac{a_{max}}{g}\frac{\sigma_v}{\sigma'_v}r_d \quad (9)$$

where the coefficient 0.65 is introduced to transform the irregular shear stress history (represented by τ_{max}) in one having an equivalent constant shear stress amplitude, σ_v and σ'_v are the vertical total and effective stresses at a depth z, a_{max} is the maximum horizontal acceleration, g is the gravity acceleration and r_d is a reduction factor accounting for soil deformability, whose expression can be found in Boulanger and Idriss (2014).

The seismic scenario assumed as a possible trigger of liquefaction was the May 20, 2012 mainshock, having moment magnitude M_w = 6.1 and epicentral distance R_{epi} = 7.5 km from the Scortichino site. An estimated maximum acceleration at the site of 0.26g, equal to the recorded value at the recording station of Mirandola (D'Amico et al. 2020), has been also adopted in the computations.

The CRR profile has been estimated following the procedure already described in section 2.

The results of liquefaction analysis are reported in Fig. 3, including also the interpretation of the CPTU profile in terms of soil behaviour type index (I_c).

The "integral" liquefaction susceptibility at each test location was evaluated using the liquefaction potential index LPI (Iwasaki et al. 1984):

$$LPI = \int_0^{20} F(z) \cdot W(z)dz \quad (10)$$

where w(z) is a depth weighting factor and the function F(z) depends on the safety factor, according to Sonmez (2003).

3.2 *Liquefaction assessment by using SDMT*

Results of liquefaction analyses based on K_D, with CRR estimated according to Eq. (8) are reported in Figure 3, including also the interpretation of the SDMT profile in terms of I_D index.

The results provided by SDMT-method indicate the possible occurrence of liquefaction (FS_{liq} <1) at local depths from the crest of the embankment between about 5 to 11 m, while no significant liquefaction is detected in the deeper sands.

The results of the analyses based on CPTU signal the presence of a liquefiable layer, having much lower thickness than indicated by K_D. Moreover, the analysis based on CPT suggests a 'moderate' liquefaction potential index, which is remarkably lower than that indicated by K_D.

The discrepancy between the two simplified analyses can be attributed to the fact that the proposed CRR correlation based on K_D (Eq. 8) is valid for clean sand or a limited number of fines (FC<10%), without any correction for fines content. Hence, the CRR estimated from K_D in the sandy-silty layers are probably somewhat underestimated, as already observed for the previous DMT-based empirical relationships (Monaco et al. 2005, Tsai et al. 2009, Robertson 2012, Marchetti 2016).

3.3 *Liquefaction assessment by using 1D dynamic analysis in effective stress*

A 1D dynamic analysis in effective stress has been performed by adopting the non-linear code SCOSSA (Tropeano et al. 2016; 2019) which models the soil profile as a system of consistent lumped masses, connected by viscous dampers and springs with hysteretic behaviour.

In the code is implemented a stress-based pore water pressure model (PWP) which permits to compare the irregular time-history of shear stress-induced by the earthquake with the soil liquefaction resistance. The comparison is expressed through the so-called 'damage parameter', which can be computed for any loading pattern. The damage parameter, κ, is an incremental function of the applied load that takes into account the cyclic strength of the soil (Chiaradonna et al. 2018).

The cyclic strength is expressed in terms of the cyclic resistance curve, which univocally relates the number of cycles at liquefaction, N_L, to the cyclic resistance ratio, CRR. The model analytically describes the cyclic resistance curve by the following equation:

$$\frac{(CRR - CSR_t)}{(CSR_r - CSR_t)} = \left(\frac{N_r}{N_L}\right)^{\frac{1}{\alpha}} \quad (11)$$

where (N_r, CSR_r) is a reference point, CSR_t the asymptotic value of CRR as the number of cycles tends to infinite and α is in some way related to the slope of the relationship. Further details can be found in Chiaradonna et al. (2016, 2018).

To extend the applicability of the PWP model to studies where laboratory data are not available, in this paper it is proposed to calibrate the parameters of the Eq. (11) directly from the results of conventional DMT tests.

The first step in the calibration process consists of generating a cyclic resistance curve from the proposed DMT-empirical relationship (Eq. 8).

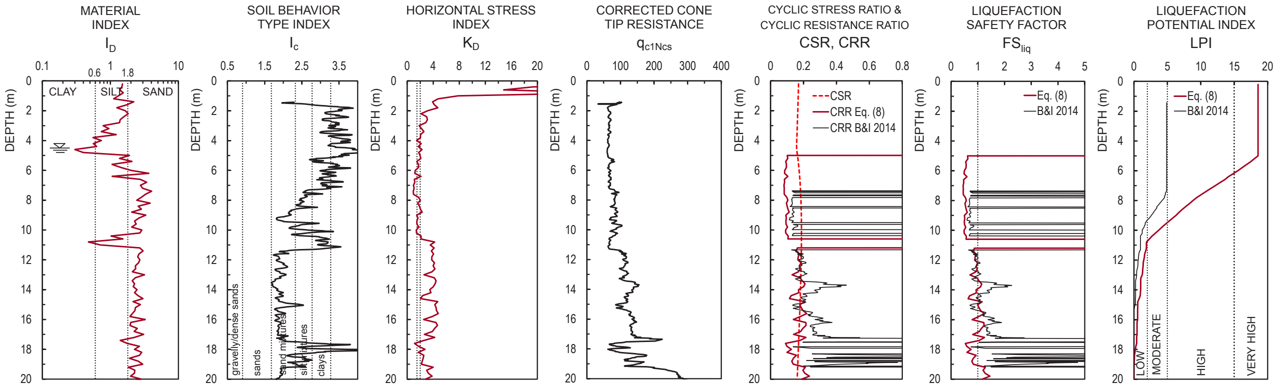

Figure 3. Results of liquefaction analyses based on the horizontal stress index K_D (SDMT) and on the cone penetration resistance q_{c1Ncs} (CPTU).

3.3.1 *Generation of cyclic resistance curves from the new empirical relationship based on DMT*

The generation procedure follows the path described by Chiaradonna et al. (2020), originally proposed for cone penetration (CPT) and standard penetration (SPT).

Indeed, each point of the empirical relationship (Eq. 8) is representative of the cyclic strength of the soil for reference magnitude of 7.5 and overburden stress equal to one. By adopting the correction factors proposed by Boulanger and Idriss (2014), already mentioned in section 2, it is possible to generate a cyclic resistance curve from a q_{c1Ncs} and, similarly from K_D for this study. For sake of brevity, all the analytical expressions are here not reported but the reader can refer to Chiaradonna et al. (2020) for details, where q_{c1Ncs} is just traced back to K_D by Eq. (7).

To assess the reliability of the generated cyclic resistance curves, a comparison has been carried out with the measured cyclic strength of the soils tested in the laboratory by direct simple shear tests, CSS (Tonni et al. 2015, Porcino and Diano 2016).

Figure 4 reports the cyclic resistance curve of clean sand deposits (A200) as measured by direct simple shear tests (CSS) at an initial confining vertical stress of 100 kPa and the predicted ones by the DMT-empirical relationship (Eq. 8) for a K_D=4 (estimated from Figure 3) and a vertical effective stress of 100 kPa and 250 kPa. Due to the consideration that the laboratory data are obtained under one-directional loading, while the empirical curves take into account the tri-directionality of the real shaking, a correction factor of 0.9 has been applied to the CRR obtained by a laboratory test, according to Kramer (1996).

For the same initial effective stress state, the empirical cyclic resistance curve slightly under predicts the soil strength, but the match is satisfied from an engineering point of view.

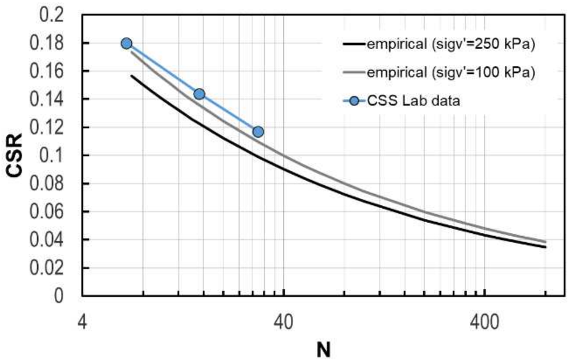

Figure 4. Comparison between the cyclic resistance curve obtained experimentally from direct simple shear tests (CSS) and the predicted ones by the empirical CRR - K_D curve for K_D=4.

3.3.2 *Input data for the 1D Dynamic analysis*

In-situ and laboratory geotechnical investigation carried out after the earthquake at the Scortichino site, allowed the definition of an accurate subsoil model for the dynamic analyses (Tonni et al. 2015, Chiaradonna et al. 2016, 2019). Figure 5 shows the soil layering and the related shear wave velocity profile, as obtained by analyzing the borehole logs and geophysical tests. The core of the dike (AR) and its foundation soil (B) consist of silty sand, while a thick formation of alluvial sands (A), interbedded by clay (C), overlies an alternation of both materials (AL) and the bedrock.

Resonant column and cyclic simple shear tests were carried out (Tonni et al. 2015) to obtain the variation of the normalized shear modulus, G/G_0, and damping ratio, D, with the shear strain, γ, required to simulate the non-linear and dissipative soil behaviour, as reported in Chiaradonna et al. (2019).

Chiaradonna et al. (2019) performed the 1D stress dynamic analysis of the considered soil column, calibrated the PWP model on the available cyclic laboratory tests.

In the present study, the cyclic resistance curve of the alluvial sand (A) has been carried out on the empirical curve of Figure 4 for confining vertical stress of 250 kPa, which corresponds to the mean initial effective stress state in soil deposit A200.

The parameters of the cyclic resistance curve used in the present study are reported in Table 1 and compared with those obtained by assuming the laboratory data in the calibration (Chiaradonna et al. 2019).

Table 1. Parameters of the cyclic resistance curve of the PWP model.

Parameter	α	CSR_t	CSR_r
Empirical curve	1.97	0.08	0.16
Lab-based curve	3.01	0.004	0.12

The deconvolved motion of the May 20, 2012 main-shock recorded at the Mirandola station (MRN) has been assumed as reference input motion for the analysis (Chiaradonna et al. 2019). The input was applied as an outcrop motion at the bedrock, which was modelled as a deformable medium with shear wave velocity V_S = 800 m/s.

3.3.2 *Results of the 1D Dynamic analysis*

The results of the effective stress analysis are reported in Figure 5 in terms of vertical profiles of the maximum excess pore pressure ratio, defined as the ratio between the pore pressure build-up induced by the shaking and the initial effective vertical stress, r_u. Figure 5 reports also the vertical r_u profile obtained by Chiaradonna et al. 2019, where the cyclic strength of the clean sand (A200) was directly defined on the cyclic laboratory test results.

As expected, the analysis where the cyclic strength of the A200 sand is based on the empirical curve (Fig. 4) provides an overestimation of the thickness of the liquefiable layer compared to the laboratory-based calibration of the cyclic strength (Fig. 5).

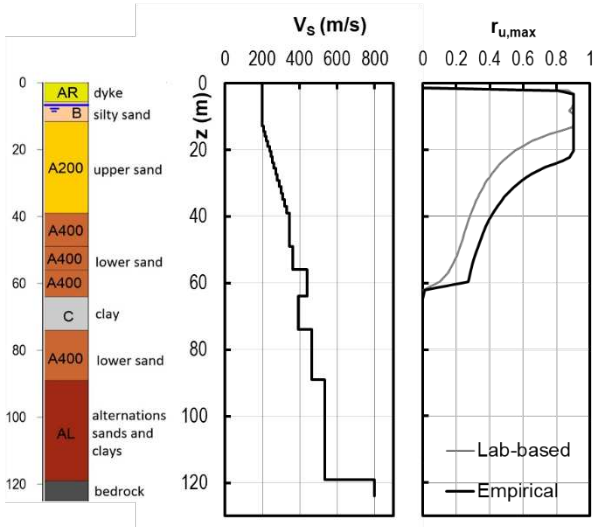

Figure 5. Vertical profile of the shear wave velocity and the maximum excess pore pressure ratio obtained by the dynamic analyses in effective stress.

4 CONCLUSIONS

This paper proposed an updating of the DMT-based empirical relationship, adopting the framework providing by Boulanger and Idriss (2014). The performance of the proposed curve was assessed on an Italian case study: a sketch of a river dyke highly damaged by the 2012 Emilia Earthquake. Liquefaction simplified analyses were performed by using both CPT and SDMT available for the considered site.

The proposed K_D-based empirical curve was used also to calibrate a simplified model for predicting the pore water pressure build-up induced by seismic loading, following a prompt calibration process for effective stress analysis already proposed by several researchers (Ntritos and Cubrinovski 2020; Chiaradonna et al. 2020). Both methodologies highlighted high liquefaction risk for the investigated foundation soil deposits of the dyke which are also compatible with the observed damage pattern.

The main drawback of the proposed approach is still related to the lack of a correction factor for the fines content. This issue will be addressed in future studies, based on field data from different test sites.

5 ACKNOWLEDGEMENTS

This work was carried out as part of WP 'Site response analysis and liquefaction' in the framework of the research programme funded by Italian Civil Protection through the ReLUIS Consortium (ReLUIS-DPC 2019-2021). One of the authors was supported by the Italian Ministry of Research through the 'Attraction and International Mobility' project.

The experimental data presented in this paper were obtained as part of the activity of the AGI-RER Working Group, promoted by the Emilia-Romagna regional authority in cooperation with the Italian Geotechnical Society.

6 REFERENCES

Amoroso S., Milana G., Rollins K.M., Comina C., Minarelli L., Manuel M.R., Monaco P., Franceschini M., Anzidei M., Lusvardi C., Cantore L., Carpena A., Casadei S., Cinti F.R., Civico R., Cox B.R., De Martini P.M, Di Giulio G., Di Naccio D., Di Stefano G., Facciorusso J., Famiani D., Fiorelli F., Fontana D., Foti S., Madiai C., Marangoni V., Marchetti D., Marchetti S.L., Martelli L., Mariotti M., Muscolino E., Pancaldi D., Pantosti D., Passeri F., Pesci A., Romeo G., Sapia V., Smedile A., Stefani M., Tarabusi G., Teza G., Vassallo M. and Villani F. 2017. The first Italian blast-induced liquefaction test (Mirabello, Emilia-Romagna, Italy): description of the experiment and preliminary results. *Annals of Geophysics*, 60 (5), Article No. S0556. https://doi.org/10.4401/ag-7415.

Amoroso S., Monaco P., Rollins K.M., Holtrigter M. and Thorp A. 2015. Liquefaction assessment by seismic dilatometer test (SDMT) after 2010-2011 Canterbury earthquakes (New Zealand). *Proc. 6th Int. Conf. on Earthquake Geotech. Eng. 6ICEGE*, Christchurch, New Zealand, Paper No. 164.

Amoroso S., Monaco P., Vargas-Herrera L.A. and Coto-Loría M. 2014. Comparison of CPTu and SDMT after 2012 Samara Earthquake, Costa Rica: liquefaction case studies. *Proc. 3rd Int. Symp. on Cone Penetration Testing CPT'14*, Las Vegas, USA, 1151-1159.

Amoroso S., Rollins K.M., Andersen P., Gottardi G., Tonni L., García Martínez M.F., Wissmann K., Minarelli L., Comina C., Fontana D., De Martini, P.M., Monaco, P., Pesci, A., Sapia, V., Vassallo, M., Anzidei M., Carpena A., Cinti F., Civico R., Coco I., Conforti D., Doumaz F., Giannattasio F., Di Giulio G., Foti S., Loddo F., Lugli S., Manuel M.R., Marchetti D., Mariotti M., Materni V., Metcalfe B., Milana G., Pantosti D., Pesce A., Salocchi A.C., Smedile A., Stefani M., Tarabusi G. and Teza G. 2020. Blast-induced liquefaction in silty sands for full-scale testing of ground improvement methods: Insights from a multidisciplinary study. *Engineering Geology* 265, Article No. 105437. https://doi.org/10.1016/j.enggeo.2019.105437.

Amoroso S., Rollins K.M., Monaco P., Holtrigter M. and Thorp A. 2018. Monitoring Ground Improvement Using the Seismic Dilatometer in Christchurch, New Zealand. *Geotech. Test. J.* 41 (5), 946-966. https://doi.org/10.1520/GTJ20170376.

Andrus R.D. and Stokoe K.H. II. 2000. Liquefaction resistance of soils from shear-wave velocity. *J. Geotech. Geoenviron. Eng.* 126(11): 1015-1025.

Boncio P., Amoroso S., Vessia G., Francescone M., Nardone M., Monaco P., Famiani D., Di Naccio D., Mercuri A., Manuel M.R., Galadini F. and Milana G. 2018. Evaluation of liquefaction potential in an intermountain Quaternary lacustrine basin (Fucino basin, central Italy). *Bulletin of Earthquake Engineering*, 16 (1), 91-111. https://doi.org/10.1007/s10518-017-0201-z.

Boulanger R.W. and Idriss I.M. 2014. CPT and SPT liquefaction triggering procedures. Report No UCD/GCM-14/01, University of California at Davis, California, USA.

Chiaradonna A. Flora A. d'Onofrio A. and Bilotta E. 2020. A pore water pressure model calibration based on in-situ test results. *Soils and Foundations* https://doi.org/10.1016/j.sandf.2019.12.010.

Chiaradonna A. Tropeano G. d'Onofrio A. and Silvestri F. 2018. Development of a simplified model for pore water pressure build-up induced by cyclic loading. *Bulletin of Earthquake Engineering* 16(9), 3627–3652 https://doi.org/10.1007/s10518-018-0354-4.

Chiaradonna A. Tropeano G. d'Onofrio A. and Silvestri F. 2019. Interpreting the deformation phenomena of a levee damaged during the 2012 Emilia earthquake. *Soil Dynamic and Earthquake Engineering* 124, 389–398 doi.org/10.1016/j.soildyn.2018.04.039

Chiaradonna A. Tropeano G. d'Onofrio A. and Silvestri F. 2016. A simplified method for pore pressure buildup prediction: from laboratory cyclic tests to the 1D soil response analysis in effective stress conditions. *Procedia Engineering* 158: 302-307. doi: 10.1016/j.proeng.2016.08.446

D' Amico M. Felicetta C. Russo E. Sgobba S. Lanzano G. Pacor F. Luzi L 2020. Italian Accelerometric Archive v 3.1 - Istituto Nazionale di Geofisica e Vulcanologia, Dipartimento della Protezione Civile Nazionale. doi: 10.13127/itaca.3.1

Iwasaki T., Arakawa T. and Tokida K. 1984. Simplified Procedures for assessing soil liquefaction during earthquakes. *Soil Dynamics and Earthquake Engineering* 3(1), 49–58.

Kramer S.L. 1996. Geotechnical earthquake engineering. Prentice Hall, Upper Saddle River, NJ.

Marchetti S. 2016. Incorporating the Stress History Parameter K_D of DMT into the Liquefaction Correlations in Clean Uncemented Sands. *J. Geotech. Geoenviron. Eng.* 142 (2), 04015072. https://doi.org/10.1061/(ASCE)GT.1943-5606.0001380.

Monaco P. and Amoroso S. 2019. Review of the liquefaction cases triggered by the 2009 L'Aquila earthquake (Italy). *Proc. 7th lnt. Conf. on Earthquake Geotech. Eng. ICEGE 2019*, Rome, Italy, 4006-4013. Series Proceedings in Earth and Geosciences. CRC Press, London, UK.

Monaco P., Marchetti S., Totani G. and Calabrese M. 2005. Sand liquefiability assessment by Flat Dilatometer Test (DMT). *Proc. XVI Int. Conf. on Soil Mech. and Geotech. Eng.*, Osaka, Japan, 4, 2693-2697. Millpress, Rotterdam, The Netherlands.

Monaco P., Santucci de Magistris F., Grasso S., Marchetti S., Maugeri M. and Totani G. 2011. Analysis of the liquefaction phenomena in the village of Vittorito (L'Aquila). *Bulletin of Earthquake Engineering* 9 (1), 231-261. https://doi.org/10.1007/s10518-010-9228-0.

Monaco P., Tonni L., Gottardi G., Marchi M., Martelli L., Amoroso S. and Simeoni L. 2016. Combined use of SDMT-CPTU results for site characterization and liquefaction analysis of canal levees. *Proc. 5th Int. Conf. on Geotechnical and Geophysical Site Characterization ISC'5*, Gold Coast, Australia, 1, 615-620. Australian Geomechanics Society, Sydney, Australia.

Ntritos N. and Cubrinovski M. 2020. A CPT-based effective stress analysis procedure for liquefaction assessment. *Soil Dynamics and Earthquake Engineering* 131, 106063

Porcino D. and Diano V. 2016. Laboratory Study on Pore Pressure Generation and Liquefaction of Low-Plasticity Silty Sandy Soils during the 2012 Earthquake in Italy. *J Geotech Geoenviron Eng,* doi:10.1061/(ASCE)GT.1943-5606.0001518.

Porcino D.D., Monaco P. and Tonni L. 2019. Evaluating Seismic Behavior of Intermediate Silty Sands of Low Plasticity from Emilia Romagna, Italy. *Geotechnical Special Publication GSP 308,* 341-351. https://doi.org/10.1061/9780784482100.035.

Robertson P.K. 2012. Mitchell lecture. Interpretation of in-situ tests—Some insight. Proc. 4th Int. Conf. on Site Characterization ISC-4, 1, 3-24. Balkema, Rotterdam, Netherlands.

Sonmez H. 2003. Modification of the liquefaction potential index and liquefaction susceptibility mapping for a liquefaction-prone area (Inegol-Turkey). *Environ. Geology* 44, 862-871.

Tonni L., Gottardi G., Amoroso S., Bardotti R., Bonzi L., Chiaradonna A., d'Onofrio A., Fioravante V., Ghinelli A., Giretti D., Lanzo G., Madiai C., Marchi M., Martelli L., Monaco P., Porcino D., Razzano R., Rosselli S., Severi P., Silvestri F., Simeoni L., Vannucchi G. and Aversa S. 2015. Interpreting the deformation phenomena triggered by the 2012 Emilia seismic sequence on the Canale Diversivo di Burana banks. *Rivista Italiana di Geotecnica* 49 (2), 28-58 (in Italian).

Tropeano G. Chiaradonna A. d'Onofrio A. and Silvestri F. 2016. An innovative computer code for 1D seismic response analysis including shear strength of soils. *Géotechnique* 66(2): 95-105.

Tropeano G. Chiaradonna A. d'Onofrio A. and Silvestri F. 2019. Numerical model for non-linear coupled analysis on seismic response of liquefiable soils. *Computers and Geotechnics* 105: 211-227. https://doi.org/10.1016/j.compgeo.2018.09.008

Tsai P., Lee D., Kung G.T. and Juang C.H. 2009. Simplified DMT-based methods for evaluating liquefaction resistance of soils. *Engineering Geology* 103(1-2), 13-22 doi.org/10.1016/j.enggeo.2008.07.008.